



Track initiation using sparse radar data for low earth orbit objects

Thibaut Castaings, Florent Muller, Benjamin Pannetier, Michèle Rombaut

► To cite this version:

Thibaut Castaings, Florent Muller, Benjamin Pannetier, Michèle Rombaut. Track initiation using sparse radar data for low earth orbit objects. 63rd International Astronautical Congress, Naples, Italy, Oct 2012, Naples, Italy. hal-00916051

HAL Id: hal-00916051

<https://hal.science/hal-00916051>

Submitted on 9 Dec 2013

HAL is a multi-disciplinary open access archive for the deposit and dissemination of scientific research documents, whether they are published or not. The documents may come from teaching and research institutions in France or abroad, or from public or private research centers.

L'archive ouverte pluridisciplinaire **HAL**, est destinée au dépôt et à la diffusion de documents scientifiques de niveau recherche, publiés ou non, émanant des établissements d'enseignement et de recherche français ou étrangers, des laboratoires publics ou privés.

IAC-12-A6.1.13

TRACK INITIATION USING SPARSE RADAR DATA FOR LOW EARTH ORBIT OBJECTS

Thibaut Castaings

ONERA, France, thibaut.castaings@onera.fr

Florent Muller, Benjamin Pannetier

ONERA, France, {florent.muller, benjamin.pannetier}@onera.fr

Michèle Rombaut

GIPSA-Lab, France, michele.rombaut@gipsa-lab.grenoble-inp.fr

This paper deals with the track-initiation problem of low Earth orbit objects observed by a space surveillance radar system of wide cross-elevation, narrow elevation sized field of view. This sensor configuration involves short arcs from which no orbital state can be computed, making regular tracking techniques not applicable. However, a set of short arcs may contain enough information to deduce such a state, the main problem being to associate them due to the high number of objects and false alarms. Recently, a method to limit the association possibilities of short arcs at one revolution of interval has been proposed. In this paper, an approach to estimate the state (six orbital elements) starting from two short arcs at one revolution of interval is presented, in order to enable track initiation in a multi-target tracking algorithm such as Track-Oriented Multi-Hypothesis Tracking. The method is based on the geometrical determination of four orbital elements, enabling the association of a third short arc to find the two remaining orbital elements. The following hypotheses on the ground radar are made to stick to current specifications of space surveillance systems being designed: south-oriented, monostatic, wide cross-elevation (160°), narrow elevation (2°) field of view, provides range, azimuth and elevation measurements. To simulate detections from the ground radar, we use real data from the Space-Track Two-Lines Elements, a space objects catalog provided by USSTRATCOM, combined with an SGP4 propagator. The principle of the presented approach follows three steps: First, the semi-major axis, the inclination, the right ascension of ascending node and the mean anomaly are retrieved from geometrical considerations. Then, the covariance matrix of the obtained state-vector is computed using a Monte-Carlo method, added to a suited process noise covariance matrix. The resulting distribution is propagated at the times of new observations using an unscented transform to assess their correlation. Finally, an iterative Newton-Gauss least square algorithm is used on the set of three correlated short arcs to find the values of the eccentricity and argument of perigee. The resulting state may be used in regular tracking techniques. The principle and functioning of the method on realistic simulation are presented, as well as its performance and limiting cases.

I. INTRODUCTION

Over time, space-based applications (such as space-based telecommunication, observation, navigation, etc.) have become essential for mankind to such an extent that their possible loss or even inability to access space would imply severe aftermath. As a consequence, the environment-related risks for space systems should be assessed and controlled. Following recent events, space debris tracking and cataloguing for collision avoidance has become a topic of great interest. For the Low Earth Orbits (LEOs), radar-based surveillance sensors exist. Aiming at ever better performance – especially cataloguing ever smaller and more numerous objects, with a higher accuracy – current sensors and methods are pushed to their limits. The best trade-off criterion for detecting smaller objects is to increase the frequency of the emitted radio-wave [KST85]. To prevent cost explosion, a reduced Field Of View (FOV), for instance a FOV of wide cross-elevation and narrow elevation (electromagnetic fence), is required. The latter option is less costly but involves short arcs (SAs), *i.e.* sparse data, of which an orbital state estimate is unavailable, excluding the use of regular techniques.

Recently, a method to limit the association possibilities of SAs at one revolution of interval has been proposed in [CPMR12], in order to provide a Track-Oriented Multiple Hypothesis Tracking algorithm (TO-MHT) [BP99] with two-SA tracks that should contain sufficient information to compute a state and start regular tracking. In [CPMR12], observations at one revolution of interval are correlated, starting from a set of behavioural features extracted from a simulation using a Space-Track Two-Lines Element (TLEs) catalog. In this paper, starting from two SAs at one revolution of interval, an approach to estimate initial orbits of six orbital elements with sufficient precision to track objects is presented.

We first briefly describe in Section II the LEO population as well as the working hypotheses. Then, the proposed method is presented in Section III. Finally, we assess its performance and discuss the results in Section IV and Section V.

II. POSITIONING

The Space-Track TLE catalog contains more than 15,000 objects with a diameter greater than 10cm, and the estimated number of smaller objects is still greater [Kes91][Sta]. However, the

density of space debris is still acceptable to operators in the sense of risk management on the mid-Earth orbits and geosynchronous Earth Orbit; this is why only the LEO objects (geodesic altitude lower than 2000Km) are within the scope of this paper. An SGP4 propagator is used to simulate the trajectories of the 11,000 LEO objects contained in the TLE catalog. This model predicts the effect of perturbations caused by the Earth's five first spherical harmonics and the atmospheric drag [HR80][VCHK06], as well as other phenomena. The chosen orbital state components are given in Table 1, other parameters being set to a null value.

t	: Element Set Epoch (UTC),
n	: Mean Motion (revolutions/day), related to Semi-major axis a by Kepler's third law
e	: Eccentricity
i	: Orbit Inclination (degrees)
Ω	: Right Ascension of Ascending Node (degrees)
ω	: Argument of Perigee (degrees)
M	: Mean Anomaly (degrees)

Table 1: Description of the chosen orbital state components.

The dependance of components n, e, i, Ω, ω and M on the element set epoch t will be omitted for the sake of clarity. Let \mathbf{X}_6 refer to the state vector $[n, e, i, \Omega, \omega, M]^T$ and \mathbf{X}_4 refer to the state vector $[n, i, \Omega, M]^T$. In the sequel, we first estimate \mathbf{X}_4 in order to correlate (with however a poor precision) a sufficient number of SAs to enable the estimation of \mathbf{X}_6 .

Maneuvering satellites are of a certain size. As a consequence, we can assume that they can be handled by existing systems and that the considered LEO objects are non-maneuvering. To adhere to actual specifications of space surveillance systems currently being designed, we assume the sensor to be:

- located in the northern hemisphere (latitude 45°)
- line of sight oriented toward South with arbitrary chosen 20° of elevation, wide cross-elevation (160°), narrow elevation (2°) FOV
- Field Of View time of revisit of 10s
- provides range ρ , azimuth θ and elevation ϕ (pulsed monostatic)
- precision of $\sigma_\rho = 30m$ in range, $\sigma_\theta = 0.2^\circ$ in cross-elevation and $\sigma_\phi = 0.2^\circ$ in elevation

- a false alarm rate of 1FA/s

Note that as the sensor provides 3D positioning measurements, most of the processing may use a cartesian, inertial geocentric frame of reference.

Let Z_k be the set of observations at scan k and m_k the number of observations at scan k . Let ρ_k^j , θ_k^j and ϕ_k^j denote the range, azimuth and elevation measurements of the j -th observation \mathbf{z}_k^j of scan k ; \mathbf{R}_k^j the covariance matrix of the measurement error; σ_ρ , σ_θ , σ_ϕ the uncertainties on range, azimuth, elevation such as [1].

$$\begin{aligned} Z_k &= \{\mathbf{z}_k^j\}_{j=1..m_k} \\ \mathbf{z}_k^j &= [\rho_k^j, \theta_k^j, \phi_k^j]^T \\ \mathbf{R}_k^j &= \text{diag}(\sigma_\rho^2, \sigma_\theta^2, \sigma_\phi^2) \end{aligned} \quad [1]$$

Let $Z^{k_1, l}$ refer to the l -th sequence of m observations such as [2].

$$Z^{k_1, l} = \{\mathbf{z}_{k_1}^{j_1}, \mathbf{z}_{k_2}^{j_2}, \dots, \mathbf{z}_{k_m}^{j_m}\} \quad [2]$$

where k_1 is the time of the latest observation.

In our case, an object going through the FOV produces an SA (*i.e.* one or two observations). We assume in this study that the observations originated from a single object during one pass through the FOV can be correctly associated into SAs using *e.g.* nearest neighbour approaches. Such considerations are out of the scope of this paper, so we focus in this study on the association of SAs. Let A^k refer to the SA containing the m successive observations $\mathbf{z}_k^{j_0}, \mathbf{z}_{k-1}^{j_1}, \dots, \mathbf{z}_{k-m+1}^{j_{m-1}}$ originated from a single pass of object through the FOV as given in [3], k being the time of the latest observation.

$$A^k = \{\mathbf{z}_k^{j_0}, \mathbf{z}_{k-1}^{j_1}, \dots, \mathbf{z}_{k-m+1}^{j_{m-1}}\} \quad [3]$$

Three or more SAs are required to compute an orbital state with sufficient accuracy (*i.e.* to associate an observation with a track without any ambiguity) to track a LEO object. Knowing the high number of LEO satellites (more than 11,000 objects of diameter greater than 10cm in the Space-Track catalog, more than 100,000 objects of diameter greater than 1cm and a high false alarm (FA) rate), testing all the possible combinations is prohibitive. The method proposed in [CPMR12] limits the number of possible first-associations of SAs, providing each new track (a track containing a single SA) with a limited number of correlated SAs at one revolution of interval.

The purpose of this work is to associate a third SA using two SAs originated from the same object at one revolution of interval, in order to enable the orbital state estimation of tracks in a TO-MHT, *i.e.* not only the accuracy of the estimated state should be sufficient to associate more SAs while limiting the number of possible associations, but a score-function should assess the quality of each association.

III. PRINCIPLE OF THE NEW APPROACH

Starting from two SAs at one orbit of interval, the track initiation technique we propose follows three steps:

1. Determine a sufficient approximation of $\mathbf{X}_4 = [n, i, \Omega, M]^T$ geometrically with a covariance matrix $\mathbf{P}_{\mathbf{X}\mathbf{X},4}$.
2. Associate an SA of the opposite node (*e.g.* if the two first SAs are ascending, a descending SA is required) using an Unscented Transform (UT).
3. Solve a least-square problem using Gauss-Newton method.

The estimation through the Gauss-Newton algorithm and the association using an UT can be used for track update as well, such as shown on Figure 1.

Estimation of \mathbf{X}_4

Starting from two SAs at one orbit of interval, the mean motion n , the inclination i , the argument of the right ascension of ascending node Ω and the mean anomaly M may be retrieved geometrically, assuming that their drifts are negligible over one revolution. Let \mathbf{r}_1 and \mathbf{r}_2 be the position-vectors of an observation taken from the first SA and of an observation taken from the second SA in an inertial, geocentric frame of reference, τ the time lapse between those observations, and α the geocentric angle between \mathbf{r}_1 and \mathbf{r}_2 .

The angle α is complementary to one revolution as shown on Figure 2, so that [4] provides a fair approximation of the mean motion n .

$$n \simeq \frac{2\pi \pm \alpha}{\tau} \quad [4]$$

A large majority of LEO objects being of very low eccentricities, it is often possible to use Kepler's third law to discriminate between the two obtained

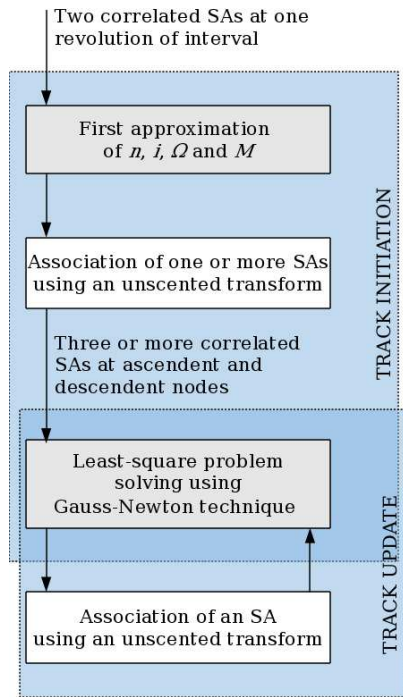


Figure 1: The track initiation step follows three steps.

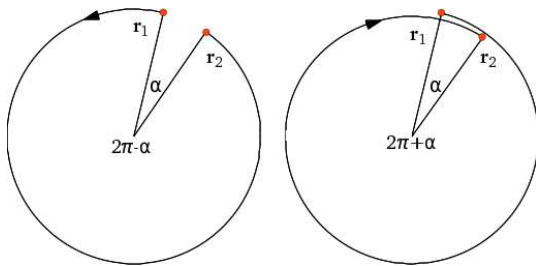


Figure 2: The object travelled less than one revolution (left). The object travelled more than one revolution (right).

values of n . If the angle α is too small to make such a choice, then both cases should be kept in memory until more SAs are added to the track.

Fair approximations of i , Ω and M are given by [5].

$$\begin{aligned}
 i &\simeq \arccos \frac{\mathbf{p} \cdot \mathbf{u}_Z}{\|\mathbf{p}\|} \\
 \text{if } \mathbf{p} \cdot \mathbf{u}_Y &\geq 0, \Omega \simeq \frac{\pi}{2} + \arccos \frac{\mathbf{p} \cdot \mathbf{u}_X}{\|\mathbf{p} \cdot \mathbf{u}_X + \mathbf{p} \cdot \mathbf{u}_Y\|} \\
 \text{else } \Omega &\simeq \frac{\pi}{2} - \arccos \frac{\mathbf{p} \cdot \mathbf{u}_X}{\|\mathbf{p} \cdot \mathbf{u}_X + \mathbf{p} \cdot \mathbf{u}_Y\|} \\
 \text{if } \mathbf{r}_1 \cdot \mathbf{u}_Z &\geq 0, M \simeq \arccos \frac{\cos \Omega \mathbf{r}_1 \cdot \mathbf{u}_X + \sin \Omega \mathbf{r}_1 \cdot \mathbf{u}_Y}{\|\mathbf{r}_1\|} \\
 \text{else } M &\simeq -\arccos \frac{\cos \Omega \mathbf{r}_1 \cdot \mathbf{u}_X + \sin \Omega \mathbf{r}_1 \cdot \mathbf{u}_Y}{\|\mathbf{r}_1\|}
 \end{aligned} \quad [5]$$

where \mathbf{p} is the cross product of \mathbf{r}_1 and \mathbf{r}_2 .

Computing several values of n , i , Ω and M using a set of randomly chosen values of \mathbf{r}_1 and \mathbf{r}_2 in the error volumes of the observations enables the calculation of a covariance matrix $\mathbf{P}_{\mathbf{X}\mathbf{X},4}$. Taking into account the accuracy of the sensor and the unavailability of the eccentricity e and argument of perigee ω at this step, we add a diagonal matrix $\mathbf{D}_{\mathbf{X}\mathbf{X},4}$ with well-chosen coefficients to $\mathbf{P}_{\mathbf{X}\mathbf{X},4}$ to reflect this additional uncertainty.

Least-square problem solving using a Gauss-Newton technique for \mathbf{X}_6 estimation

Statement 1:

The track contains at least two ascending SAs and one descending SA or two descending SAs and one ascending SA.

We propose in this paper to provide a Gauss-Newton algorithm with the values \mathbf{X}_4 in \mathbf{X}_6 as a starting point, setting the eccentricity e and the argument of perigee ω to a null value, which is relevant since a large majority of the LEO population are of low eccentricities. In practice, a track should make Statement 1 true for a Gauss-Newton algorithm to succeed in estimating its state. As a consequence, the least-square problem [6] should be solved to complete the orbital state (find the values of e and ω) as soon as Statement 1 becomes true and to refine the estimation of \mathbf{X}_6 each time a new SA is associated to an initialized track (*i.e.* a track associated to a 6-component state \mathbf{X}_6). Besides, the Gauss-Newton algorithm must also estimate a covariance matrix $\mathbf{P}_{\mathbf{X}\mathbf{X},6}$ characterizing the local minimum $\hat{\mathbf{X}}_6$, to which a diagonal matrix $\mathbf{D}_{\mathbf{X}\mathbf{X},6}$ with well-chosen coefficients may be added in difficult cases so the true state has an acceptable probability in the normal distribution defined by $\hat{\mathbf{X}}_6$ and $\mathbf{P}_{\mathbf{X}\mathbf{X},6} + \mathbf{D}_{\mathbf{X}\mathbf{X},6}$.

$$\hat{\mathbf{X}}_6 = \min_{\mathbf{X}} \sum_{j=1}^N (\bar{\mathbf{z}}^j(\mathbf{X}) - \mathbf{z}^j)^T (\mathbf{R}^j)^{-1} (\bar{\mathbf{z}}^j(\mathbf{X}) - \mathbf{z}^j) \quad [6]$$

where $\hat{\mathbf{X}}_6$ is an estimate of \mathbf{X}_6 , \mathbf{z}^j is the j -th observation available and $\bar{\mathbf{z}}^j(\mathbf{X})$ the associated prediction using the state vector \mathbf{X} . Non-linear problems such as orbital state estimation should be solved iteratively, so that the state increment $\Delta \mathbf{x}$ given by [7] is computed and added to \mathbf{X} at each iteration until a convergence criterion is reached.

$$\Delta \mathbf{x} = (\mathbf{J}^T(\mathbf{R}^j)^{-1}\mathbf{J})^{-1}\mathbf{J}^T(\mathbf{R}^j)^{-1}\mathbf{b}^j \quad [7]$$

where \mathbf{J} is the jacobian of the prediction function computed using \mathbf{X} and \mathbf{b}^j is the vector of residue, *i.e.* the concatenation of the $\{\bar{\mathbf{z}}^j(\mathbf{X}) - \mathbf{z}^j\}_j$. In our case, an attempt to solve problem [6] with too few SAs would lead to the divergence of the iterative loop or to convergence toward a wrong value (the system is not observable).

Association of SAs using an Unscented Transform

Correlating SAs with the previously defined track involves a prediction step which can be expressed such as [8], where $\bar{\mathbf{z}}_k$ is the predicted observation at time k (implicit), \mathbf{X} the state associated to the track and f the prediction function.

$$\bar{\mathbf{z}}_k = f(\mathbf{X}, k) \quad [8]$$

The principle of the UT [JUDW95] is to select a set of so-called sigma-points (*i.e.* points which have the same statistical features than the prior \mathbf{X}) and to retrieve the distribution of $\bar{\mathbf{z}}_k$ from the propagated sigma-points, such as shown on Figure 3. The UT can handle any non-linearity and is faster than a method requiring the computation of a jacobian in our case.

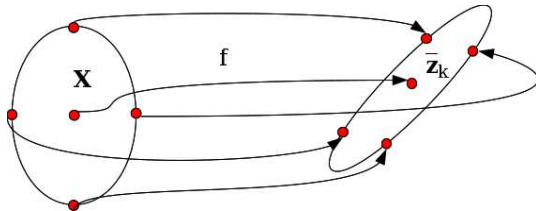


Figure 3: The distribution of $\bar{\mathbf{z}}_k$ is retrieved from the propagation of sigma-points through f .

Correlation between a track and an observation may be assessed using a χ^2 criterion on the innovation $\tilde{\mathbf{z}}_k$, such as [9], where $\mathbf{P}_{\bar{\mathbf{z}}\bar{\mathbf{z}},k}$ is the covariance matrix of the predicted distribution of \mathbf{z}_k , \mathbf{R}_k the covariance matrix of the observation noise, $\bar{\mathbf{z}}_k$ is the mean of the predicted distribution, \mathbf{z}_k is the observation, and d^2 is a distance measurement following a χ^2 distribution with three degrees of liberty in our case (3-dimensional observations).

$$\begin{aligned} \tilde{\mathbf{z}}_k &= \bar{\mathbf{z}}_k - \mathbf{z}_k \\ d^2 &= \tilde{\mathbf{z}}_k^T (\mathbf{P}_{\bar{\mathbf{z}}\bar{\mathbf{z}},k} + \mathbf{R}_k)^{-1} \tilde{\mathbf{z}}_k \end{aligned} \quad [9]$$

The value of d^2 may be compared to the cumulative density function of a χ^2 distribution to

decide whether the observation is correlated to the track. The value of d^2 may also be used to compute a log-likelihood increment ΔL to assess the quality of the association, given by [10], where C is a constant depending on the sensor features and $|\cdot|$ denotes the determinant.

$$\Delta L = \ln \frac{C}{\sqrt{|\mathbf{P}_{\bar{\mathbf{z}}\bar{\mathbf{z}},k} + \mathbf{R}_k|}} - \frac{d^2}{2} \quad [10]$$

The UT may be used to associate new SAs to existing tracks starting from \mathbf{X}_4 and $\mathbf{P}_{\mathbf{X}\mathbf{X},4}$ or \mathbf{X}_6 and $\mathbf{P}_{\mathbf{X}\mathbf{X},6}$.

IV. PERFORMANCE

Since the technique we propose and investigate in this paper aims at providing a TO-MHT with initialized tracks in a frame of high detection density, the number of correlated SAs at each association step, as well as the relevance of the score-function, are criteria of interest.

To assess the performance of the technique, we run a 3-days simulation using real data from the Space-Track TLE catalog combined with an SGP4 propagator. The simulated detections (including FAs) from a ground-based radar sensor configuration described in Section II are processed with the first-association technique proposed in [CPMR12] in order to form two-SA tracks. We apply the technique described in the paper starting from the resulting two-SA tracks and extract the following figures from the correct associations.

The distribution of the number of SAs correlated to a track using a 4-component orbital state \mathbf{X}_4 and $\mathbf{P}_{\mathbf{X}\mathbf{X},4}$ (*i.e.* before least-square solving) is presented in Figure 4. The distribution of the number of SAs correlated to a track using a 6-component orbital state \mathbf{X}_6 and $\mathbf{P}_{\mathbf{X}\mathbf{X},6}$ (*i.e.* after least-square solving) is presented in Figure 5. Very high values (greater than 100) are not taken into account in the performance assessment as they correspond to rare difficult cases.

The score increment against the length of the track is presented in Figure 6 and the score against the length of the track (cumulative integral of the score increment) is presented in Figure 7. Low (smaller than -15) score increments correspond to rare cases (0.6%). On the mean, a track becomes suitable for least-square solving when it contains 3.74 SAs. Figure 6 shows that the score increment is relatively small before least-square solving whereas it is relatively high after least-square solving. As a consequence, the score of a correct track

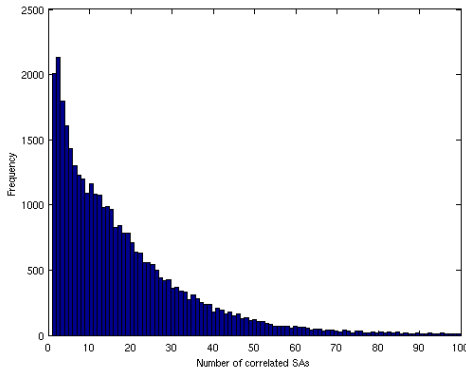


Figure 4: Distribution (Mean = 17.71) of the number of SAs correlated to a track using a 4-component orbital state \mathbf{X}_4 and $\mathbf{P}_{\mathbf{X}\mathbf{X},4}$.

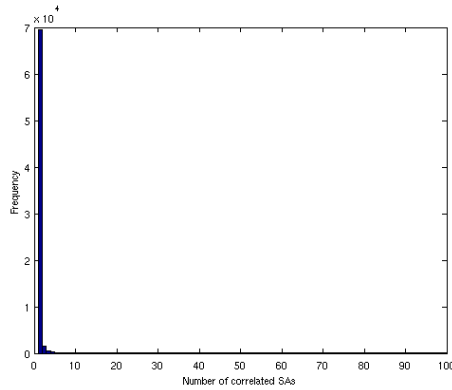


Figure 5: Distribution (Mean = 1.10) of the number of SAs correlated to a track using a 6-component orbital state \mathbf{X}_6 and $\mathbf{P}_{\mathbf{X}\mathbf{X},6}$.

does not vary significantly until the Gauss-Newton algorithm reaches convergence.

V. DISCUSSION

It appears that the state estimated from solving the least-square problem with respect to Statement 1 provides a 6-component state (*i.e.* \mathbf{X}_6 and $\mathbf{P}_{\mathbf{X}\mathbf{X},6}$) accurate enough to enable the sequence to correlate with a single SA in more than 94% of the cases, as opposed to the state estimated geometrically (*i.e.* \mathbf{X}_4 and $\mathbf{P}_{\mathbf{X}\mathbf{X},4}$) which enables a sequence to correlate with less than 50 SAs in more than 94% of the cases. As a consequence, the orbital state of an object may be estimated with sufficient precision to make categoric associations as soon as the minimum Statement 1 is true. Although several tens of SAs

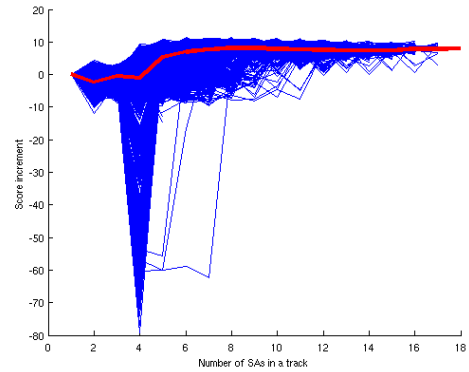


Figure 6: Score increment against length of the track. 20,724 track score increments are plotted with blue, fine lines, their mean is plotted with a red, bold line. On the mean, a step happens between the fourth and the fifth SA.

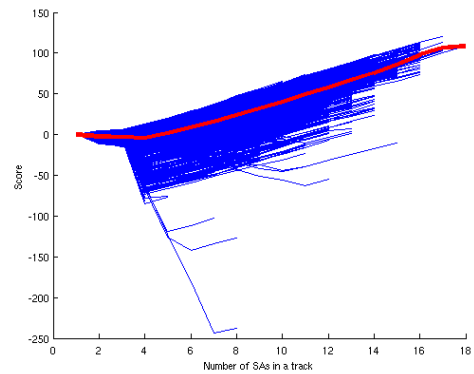


Figure 7: Score against length of the track. 20,724 track scores are plotted with blue, fine lines, their mean is plotted with a red, bold line.

may be correlated to a track until then, the use of \mathbf{X}_4 and $\mathbf{P}_{\mathbf{X}\mathbf{X},4}$ avoids testing all the possible combinations between tracks and SAs, which is valuable in a Multi-Target Tracking (MTT) frame.

The score evolution scheme suggests that it cannot be used to discriminate correct tracks and wrong tracks until Statement 1 becomes true, whereas it provides a very reliable track quality assessment afterwards.

VI. CONCLUSION

In this paper, we proposed and investigated a new technique to initialize tracks in an MTT frame for LEO objects tracking using an electromagnetic fence, involving a very high number of objects and

false alarms which makes the combinatory prohibitive if all the possible associations have to be tested. Starting from the output of an algorithm previously published in [CPMR12], the technique presented in this paper enables the computation of orbital states while directly reducing the combinatorial complexity, making scored, initialized tracks available to a TO-MHT algorithm. Moreover, the score evolution scheme may suggest leads to adapt a TO-MHT algorithm to the problem of tracking the LEO population, *e.g.* to take into account that the well-known score-function used in this study does not discriminate well between correct and wrong tracks for which Statement 1 is not true yet. This score evolution scheme also suggests that the effort to reduce the combinatory complexity should be focused on the track initiation, since near-deterministic trajectories are obtained as soon as Statement 1 becomes true.

References

- [BP99] S. Blackman and R. Popoli. *Design and Analysis of Modern Tracking Systems*. Artech House Radar Library, 1999.
- [CPMR12] T. Castaings, B. Pannetier, F. Muller, and M. Rombaut. Sparse data association for low earth orbit tracking. In *Aerospace Conference, 2012 IEEE*, 2012.
- [HR80] F. R. Hoots and R. L. Roehrich. Models for propagation of norad element sets, spacetrack report no. 3. Technical report, US Air Force, 1980.
- [JUDW95] S. J. Julier, J. K. Uhlmann, and H. F. Durrant-Whyte. A new approach for filtering nonlinear systems. In *Proceedings of the American Control Conference, Seattle, Washington, pages 1628-1632*, 1995.
- [Kes91] D. Kessler. Collisional cascading: The limits of population growth in low earth orbit. *Advances in Space Research*, 1991.
- [KST85] E. F. Knott, J. F. Shaeffer, and M. T. Tuley. *Radar Cross Section*. Artech House Radar Library, 1985.
- [Sta] E. G. Stansbery. Growth in the number of ssn tracked orbital objects. In *IAC-04-IAA.5.12.1.03*.

- [VCHK06] D. A. Vallado, P. Crawford, R. Hujsak, and T. S. Kelso. Revisiting spacetrack report no. 3. Technical report, American Institute of Aeronautics and Astronautics, 2006.